SLAC-PUB-6113
DOE/ER/40762-009
U of Md. PP #93-198
May 1993
T/E

QED-Induced Rapidity-Gap Events at the Z Peak*

HUNG JUNG LU

Department of Physics, University of Maryland

College Park, Maryland 20742, U.S.A.

STANLEY J. BRODSKY

Stanford Linear Accelerator Center

Stanford University, Stanford, California 94309, U.S.A.

and

VALERY A. KHOZE

Department of Physics, University of Durham

Durham DH1 3LE, ENGLAND

Submitted to *Physics Letters B*

---

* Supported in part by Department of Energy contract DE-AC03-76SF00515 (SLAC) and contract DE-FG02-93ER-40762 (Maryland), and by the United Kingdom Science and Engineering Research Council (Durham).

ABSTRACT

We study rapidity-gap events in e^+e^- annihilation at the Z boson peak initiated by the emission of a virtual photon. This mechanism is suppressed by the QED coupling constant, but it is enhanced due to a large propagator term from the virtual photon. For typical kinematics, we find a smaller event rate than analogous QCD type gap events. In the small jet-pair invariant mass limit, the QED type events follow a $1 + \cos^2\theta$ distribution in the jet-pair scattering angle, instead of the $\sin^2\theta$ distribution of the QCD case.

Jet events observed at e^+e^- annihilation can be understood as the creation of short-distance quarks and gluons which subsequently materialize into hadrons. As the short-distance colored particles move apart, the rapidity region separating the colored objects is filled by the hadrons. However, as pointed out in Refs. [1,2], a perturbative QCD mechanism exists which generates jet events containing rapidity gaps. The representative diagrams are shown in Fig. 1. Essentially, two color-singlet collinear jet pairs are produced at short distance. The production of hadrons is expected to be suppressed in the rapidity gap region separating the two color-singlet systems. This QCD mechanism is found to give an observable rate at Z-peak for producing gap events [3]. Qualitatively, the rapidity gap events constitute a fraction

$$R_{\rm gap}^{\rm QCD} = \sigma_{\rm gap}^{\rm QCD}/\sigma_{\rm tot} \sim \alpha_s^2 \frac{M_1^2}{s}\,\frac{M_2^2}{s} \tag{1}$$

of the total Z cross section, where M_1^2 and M_2^2 are the invariant mass of the jet pairs.

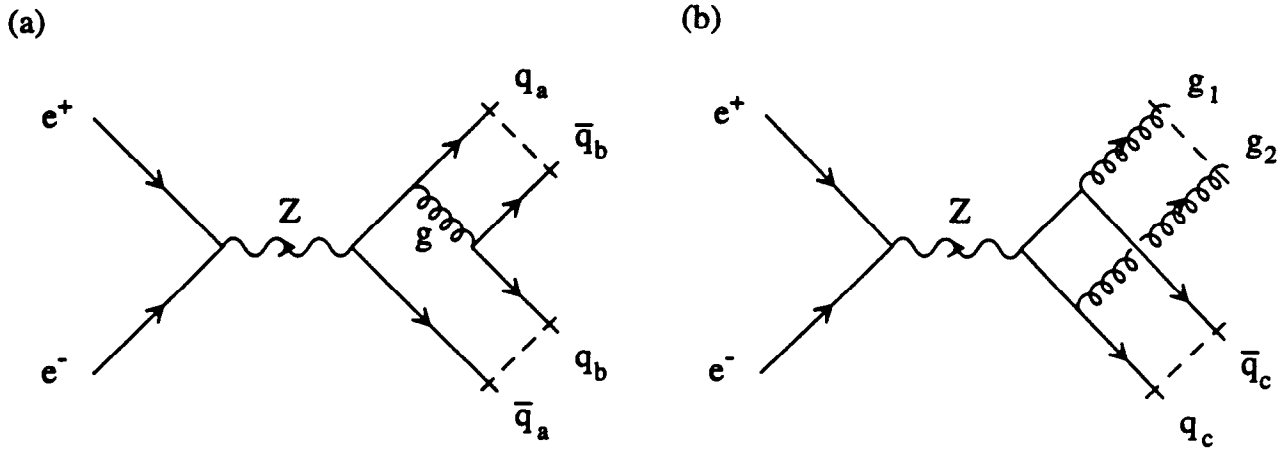

Figure 1. Perturbative QCD mechanisms for generating rapidity gap events. The dashlines indicate that the produced partons are in color-singlet state. (a) Two final-state quark-antiquark pairs. (b) A quark-antiquark jet-pair and a two-gluon jet-pair.

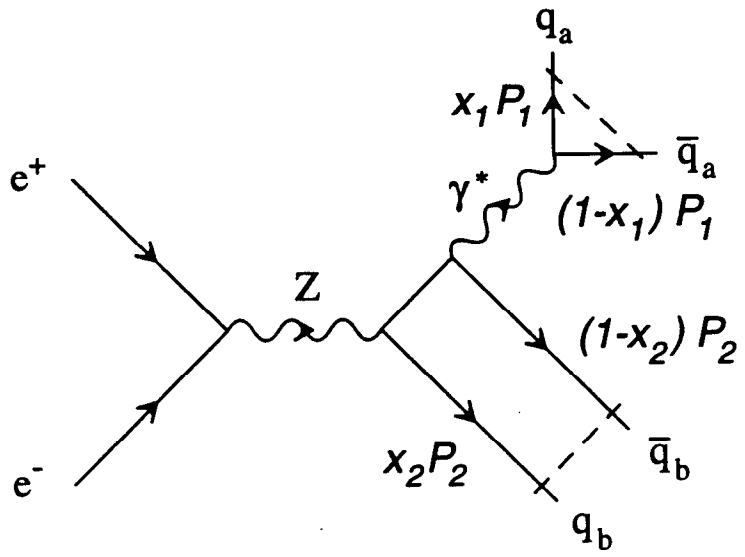

Figure 2. A QED mechanism for generating rapidity gap events. The variables x_1 and x_2 are the momentum fractions carried by the quark inside each jet-pair. The dashlines indicate that the produced quark and antiquark are in color-singlet state.

The recent interest in the study of events containing rapidity gaps has been motivated by the use of these events as possible triggering signals in high-mass scale physics [1,4,5,6]. In this article, we shall study an interesting QED mechanism that contributes additionally to the generation of rapidity-gap events in e^+e^- annihilation at Z peak. One possibility is to replace the gluon propagator in Fig. 1(a) by a photon propagator. This contribution has an identical kinematic dependence of the analogous QCD process, but it is suppressed due to the smallness of the QED coupling constant. In Fig. 2 we show the Feynman diagram in an alternative configuration, where one of the color-singlet jet-pairs is effectively the decay product of a virtual photon. There is no QCD analogy for this configuration since the gluon is a color octet object. Although the new contribution is still suppressed by α_{em}^2, the virtual photon propagator can substantially compensate for the coupling constant suppression. In fact, for small invariant-mass jet-pairs, the

diagram in Fig. 2 acquires a large enhancement due to the small virtuality carried by the photon. This should be contrasted with the QCD diagram in Fig. 1(a), where the quark and antiquark produced by the virtual gluon are required to go in opposite directions across the rapidity gap, so that the virtuality carried by the gluon is generally large.

From power counting we expect the QED rapidity gap events to be produced at a rate given by

$$R_{\rm gap}^{\rm QED} = \sigma_{\rm gap}^{\rm QED}/\sigma_{\rm tot} \sim \alpha_{em}^2 \frac{M_2^2}{s}. \tag{2}$$

That is, compared to the QCD case of Eq. (1), the event rate is enhanced by a power of s/M_1^2, despite the suppression in the coupling constant. In fact, for typical kinematics, the QED contribution can become as large as the $q\bar{q}gg$ contribution of the QCD case (Fig. 1(b)). (In Ref. [1] we have shown that the $q\bar{q}q\bar{q}$ contribution of Fig. 1(a) is about an order of magnitude larger than the $q\bar{q}gg$ contribution.) In principle, the QED diagrams interfere with the QCD diagrams when the quark jets have identical flavor. However, as we shall see, in the small invariant mass limit, the interference effects become unobservable when we integrate over the azimuthal angle of the individual jets with respect to the thrust axis of the jet-pairs. In particular, this interference has no effect on the total cross section. The QED and QCD contributions to the event rate can therefore be calculated separately.

As in Ref. [1], we will neglect quark masses and consider the small jet-pair invariant mass limit: $M_1^2, M_2^2 \ll s$. The kinematic variables are as specified in Fig. 2, where P_1 and P_2 are the four momentum of the jet pairs, and x_1, $1-x_1$, x_2, $1-x_2$ are the momentum fractions of the individual jets inside the jet pairs. We

define the two-component weak charge of a fermion to be [1]

$$\mathbf{Q}_f = \begin{pmatrix} Q_f^L \\ Q_f^R \end{pmatrix} = \begin{pmatrix} \sec\theta_{\rm w} I_f - \sin\theta_{\rm w}\tan\theta_{\rm w} Q_f \\ -\sin\theta_{\rm w}\tan\theta_{\rm w} Q_f \end{pmatrix}, \tag{3}$$

where $\theta_{\rm w}$ is the weak angle, I_f the isospin and Q_f the electric charge of the fermion f. Using this notation, the total e^+e^- annihilation cross section around the Z resonance can be conveniently expressed as:

$$\sigma_Z = \frac{\pi}{3}\frac{\mathbf{Q}_e^2\mathbf{Q}_Z^2\alpha_{\rm w}^2\ s}{(s-M_Z)^2+\Gamma_Z^2 M_Z^2}, \tag{4}$$

where

$$\begin{aligned} \mathbf{Q}_Z^2 &= \sum_f \mathbf{Q}_f^2 = \sum_l \mathbf{Q}_l^2 + 3\sum_q \mathbf{Q}_q^2 \simeq 3.771 \\ &(l = e,\mu,\tau; q = u,d,c,s,b), \\ \mathbf{Q}_f^2 &= Q_f^{L\,2} + Q_f^{R\,2}, \\ \alpha_{\rm w} &= \frac{g_{\rm w}^2}{4\pi} = \frac{e^2}{4\pi\sin^2\theta_{\rm w}} \simeq \frac{1}{29.3}, \\ M_Z, \Gamma_Z &= \text{ mass and width of the } Z \text{ boson.} \end{aligned} \tag{5}$$

We shall later use this cross section to normalize the production rate of rapidity-gap events. This is subject to the same caveat pointed out in Ref. [1]. Namely, initial state radiation induces a substantial correction to the above result for σ_Z [7]. However, the same effect is present in rapidity-gap events; thus we expect these effects to largely cancel when we consider ratios of cross sections.

There are three additional Feynman diagrams contributing to QED rapidity gap events similar to the one depicted in Fig. 2. Basically, there are two diagrams with the virtual photon decaying into $q_a\bar{q}_a$ and another two diagrams with the virtual photon decaying into $q_b\bar{q}_b$. The intermediate formulas in the calculation of

the helicity amplitudes are complicated and will not be presented here. However, we shall display a particular helicity amplitude in order to facilitate later discussion. Let us momentarily add up the contributions of the two Feynman diagrams with the virtual photon decaying into $q_a\bar{q}_a$ and designate this sum by $i\mathcal{M}^a$. Keeping only leading contribution in the jet-invariant mass M_1, we obtain the following amplitude for all-positive fermion helicities (one right-handed electron line and two right-handed quark lines):

$$i\mathcal{M}^a(+++) = \frac{4g_{\rm w}^2 e^2 Q_e^R Q_a^R Q_a Q_b \sqrt{s}}{(s - M_Z^2 + i\Gamma_Z M_Z)M_1} \left\{(1-x_1)\sqrt{\frac{x_2}{1-x_2}}\cos^2(\theta/2)e^{i\phi_1} - x_1\sqrt{\frac{1-x_2}{x_2}}\sin^2(\theta/2)e^{-i\phi_1}\right\}, \tag{6}$$

where $g_{\rm w}$ is the weak coupling constant, θ is the polar angle of the jet-pair thrust axis, and ϕ_1 is the azimuthal angle of the q_a jet with respect to the thrust axis. The sum of the other two amplitudes where the virtual photon decays into $q_b\bar{q}_b$ can be obtained by interchanging $a \leftrightarrow b$, $x_1 \leftrightarrow x_2$, $\phi_1 \leftrightarrow \phi_2$ in the previous formula. (We will refers to this sum as $i\mathcal{M}^b$.) Other helicity amplitudes can be deduced from the previous formula by various conjugation operations, but for simplicity we shall omit them here. Notice the presence of the $e^{\pm i\phi_1}$ dependence. This dependence on the azimuthal angle ϕ_1 is absent for the QCD amplitudes as those in Fig. 1. Therefore, the interference effect between the QED and QCD amplitudes disappear upon integration of the ϕ_1 angle. Similarly, the interference term between $i\mathcal{M}^a$ and $i\mathcal{M}^b$ disappear after integrating out ϕ_1 or ϕ_2. In short, interference effects only alter the azimuthal angle distribution of the individual jets with respect to the thrust axis, and these effects become unobservable when we integrate out those azimuthal angles.

The difference in the azimuthal angle dependence in QED and QCD is related the following fact. In the QCD case, the outgoing parton pairs can be perfectly aligned. In this collinear limit the azimuthal angles of the individual jets with respect to the thrust axis are not expected to play a role in the scattering amplitude. In the QED case, the jets originated from the virtual photon are forbidden to be exactly parallel, since a timelike virtual photon with helicity ± 1 cannot decay into two parallel, massless quarks: some non-collinearity is required in order to carry the photon's polarization. The appearance of the azimuthal dependence reflects the correlation between the outgoing jets with the event plane formed by the virtual photon and the beam direction.

Considering only $i\mathcal{M}^a$, after squaring, averaging and adding the various helicity contributions, counting the color multiplicity of the quarks, symmetrizing the momentum fraction variables, integrating out the azimuthal angle ϕ_1, and normalizing the cross section with respect to the total Z cross section, we obtain

$$\begin{aligned}\frac{\sigma_a}{\sigma_Z} = \frac{27}{32}\left(\frac{\alpha_{em}}{\pi}\right)^2 \frac{Q_a^2 Q_b^2 \mathbf{Q}_b^2}{\mathbf{Q}_Z^2} \int \frac{dM_1^2}{M_1^2}\,\frac{dM_2^2}{s}\, dx_1\, dx_2\, d\cos\theta \\ \times \left[x_1^2 + (1-x_1)^2\right]\left[\frac{x_2}{1-x_2} + \frac{1-x_2}{x_2}\right](1+\cos^2\theta)\ .\end{aligned} \tag{7}$$

Notice first the $1 + \cos^2\theta$ term in the above formula. This angular dependence differs from the $\sin^2\theta$ distribution obtained for QCD induced gap events. In particular, the QED type events can become the dominant contribution for polar angles near the forward and backward beam direction. Notice also the integral of M_1^2 has an apparently infrared divergence when $M_1^2 \to 0$. In reality this divergence does not occur due to the physical energy threshold $\widetilde{M}_a$ for the production of the quark-antiquark pair $q_a\overline{q}_a$ from a virtual photon. Numerically we will take

$\widetilde{M}_a = M_\rho,\ M_\omega,\ M_\phi,\ M_{J/\psi}$ and M_Υ as representative values for the threshold energy of producing quark-antiquark pairs of flavor u, d, s, c and b. Finally, notice the factorization of the x_1, x_2 and $\cos\theta$ dependence. Eq. (7) can therefore be interpreted as the probability of the radiative decay of Z into a quasi-collinear quark-antiquark pair and a virtual photon, multiplied by the probability of a photon "splitting" into a quasi-collinear quark-antiquark pair (represented by the $x_1^2 + (1-x_1)^2$ term in the equation). The singularity in the x_2 and $1-x_2$ denominators reflects the infrared divergence in the virtual quark propagator when its associated quark or antiquark becomes soft (See Fig. 2). However, as in the QCD case [1,2], when we impose the existence of a rapidity gap, the virtual photon and the other jet-pair are required to go in opposite direction across the rapidity gap, hence the momentum transfer of the virtual quark is generally hard and the infrared divergence is avoided.

Taking now into account contributions from $i\mathcal{M}^b$, adding over all quark flavor combinations, symmetrizing the identical flavors cases, and integrating over θ, we obtain

$$R_{\rm gap}^{\rm QED} = \left(\frac{9}{4}\right)^2 \left(\frac{\alpha_{em}}{\pi}\right)^2 \frac{\sum Q_b^2 \mathbf{Q}_b^2}{\mathbf{Q}_Z^2} \sum Q_a^2 \int\limits_{\widetilde{M}_a^2} \frac{dM_1^2}{M_1^2} \int \frac{dM_2^2}{s} \times \int dx_1 \left[x_1^2 + (1-x_1)^2\right] \int dx_2 \left[\frac{x_2}{1-x_2} + \frac{1-x_2}{x_2}\right] . \tag{8}$$

In principle, we should consider also the QED contribution from diagrams like Fig. 1(a) where the gluon propagator has been replaced by a photon propagator. These diagrams contribute mainly through interference effects with the corresponding QCD diagrams. A detailed analysis reveals that these effects are negligible. (The

resulting interference causes only a 0.6% decrease in the QCD-type event rate for the symmetric gap case.)

The limits of the various integrals in the above formula depend on the physical cuts we impose for the selection of events. As in Ref. [1], we first analyze the event rate for a symmetric gap cut case and then repeat the analysis for the asymmetric gap cut case. In the former case, we sum over all events with all the produced jets having an absolute rapidity greater than $g/2$ with respect to the jet-pair thrust axis. (This is subject to the same caveat pointed out in Ref. [1]; namely, due to the effect of hadronization process, the hadron fragments of each quark are concentrated within a circle of radius ~ 0.7 in the lego plot. The physically observed gap is thus expected to have a width $g_{\rm eff} \sim g - 1.4$.)

The QED and QCD type gap event rate per million Z events, is shown in Fig. 3 as a function of the symmetric rapidity gap cut g. In Fig. 4 we plot the event rate per million Z events when the gap is not required to be symmetric and the jet-pair invariant masses are required to be less than 30 or 15 GeV. We have used a value $\alpha_s = 0.13$ for the strong coupling constant. We see from these figures that in the large rapidity gap region the QED-induced events can constitute a substantial fraction of the QCD type events. For instance, $R_{\rm gap}^{\rm QED}/R_{\rm gap}^{\rm QCD} \sim 0.11$ for $g = 4$ in the symmetric gap case. The event rate for a larger gap region is probably too small for present experimental observation. In Ref. [1] we have pointed out that in the QCD case, the $q\bar{q}gg$ type events are suppressed by a factor 0.159 with respect to the $q\bar{q}q\bar{q}$ type events in the symmetric gap case. (This relative suppression can be understood on the basis of color factors: at large N_C the rate for color singlet production $(q\bar{q})+(gg)$ is proportional to N_C, whereas the rate for two mesonic dijets $(q\bar{q})$ $(q\bar{q})$ is of order N_C^2.) Hence the QED type events can become as important as

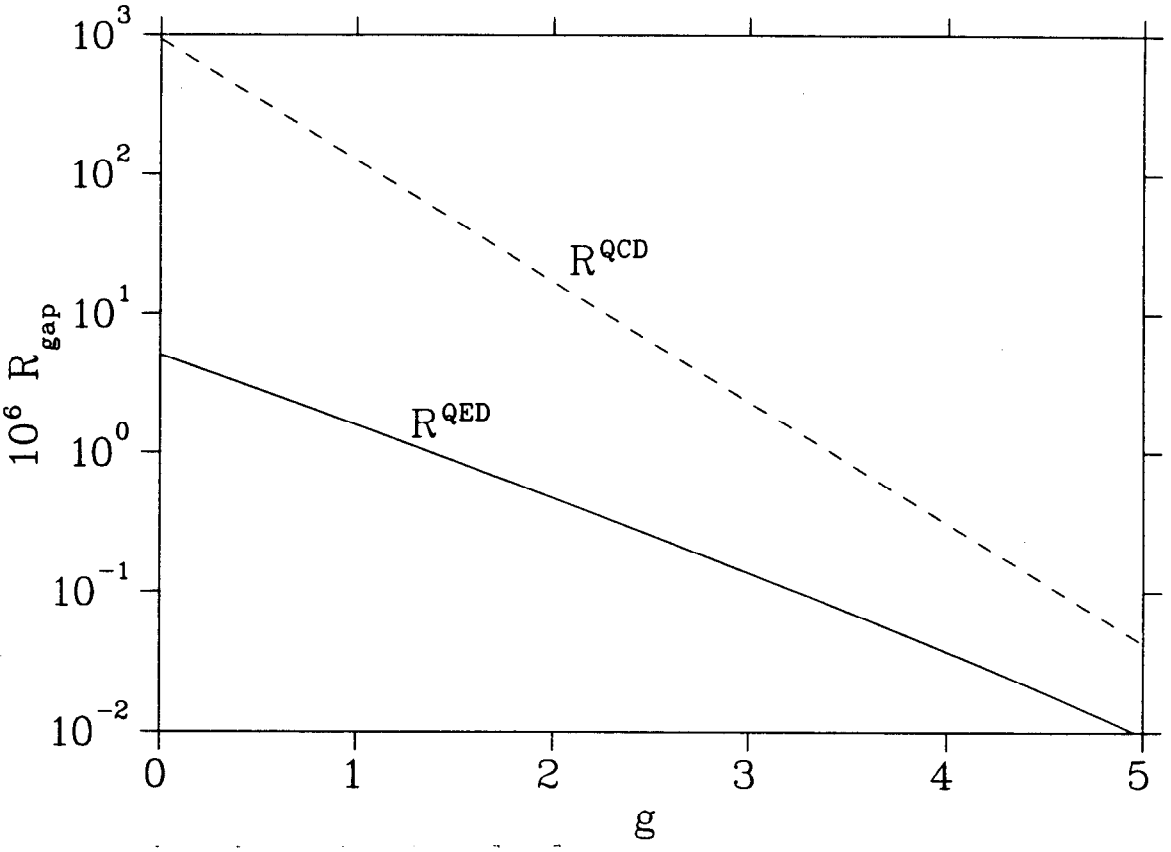

Figure 3. Rapidity gap event rate per million Z in the symmetric gap cut case, for QCD and QED.

the $q\bar{q}gg$ type rapidity gap events in the large gap region ($g \geq 4$).

In summary, we have studied QED mechanisms for producing jet event containing large rapidity gaps in e^+e^- annihilation at the Z peak energy. For typical kinematics, the event rate is found to be small compared to the rate for the corresponding QCD processes. However, the QED-induced rapidity gap events have some distinctive features. For instance, the QED events are distributed as $1+\cos^2\theta$ in terms of the polar angle θ of the thrust axis as opposed to the QCD events which are distributed as $\sin^2\theta$. The QCD and QED mechanism also favor different flavor combinations. A process involving a $(b\bar{b})$ and $(c\bar{c})$ color singlet jet-pair is clearly

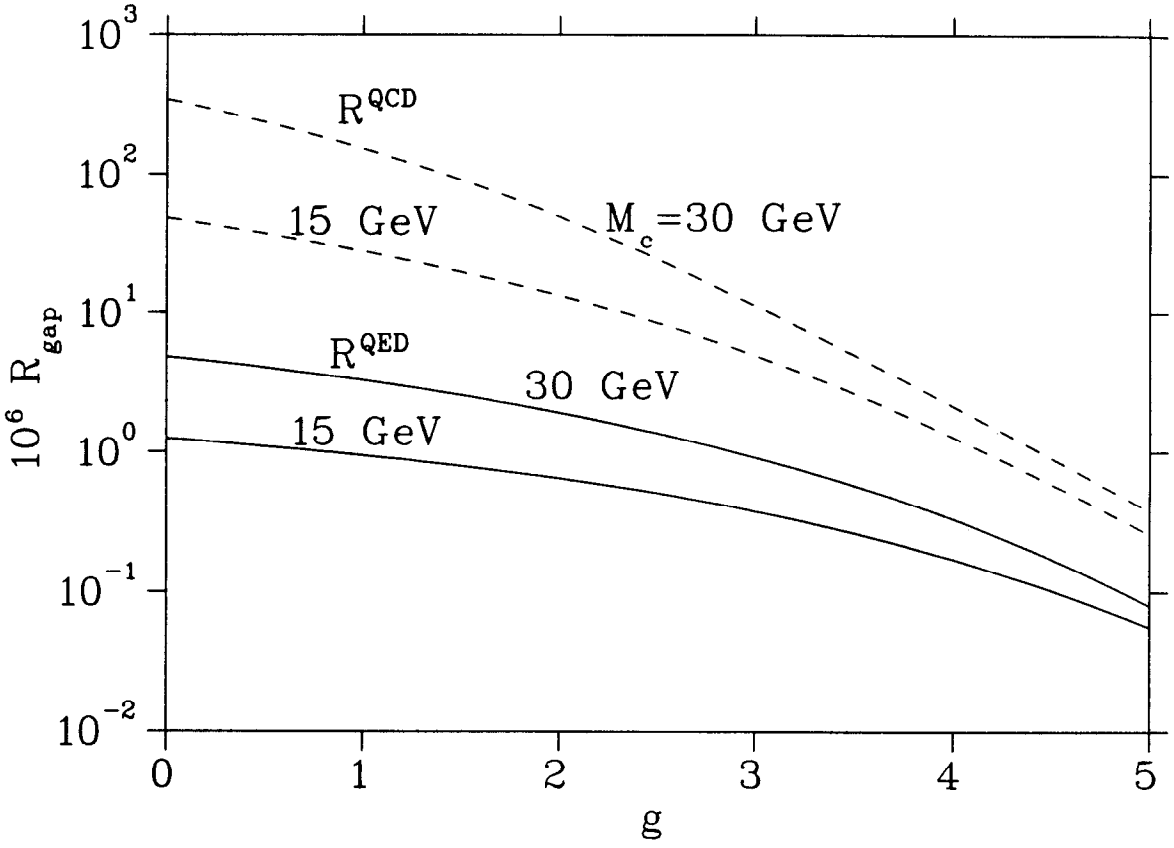

Figure 4. Rapidity gap event rate per million Z in the asymmetric gap cut case, for two different values of jet-pair invariant-mass cut (M_c = 30 GeV and M_c = 15 GeV). The dashed lines are the event rates for QCD-induced gap events, and the solid lines are for QED-induced gap events.

absent in the QCD $q\bar{q}q\bar{q}$ mechanism. Also, in the QED case, one of the jet-pairs tends to have a small invariant mass. In fact, the virtual photon easily transforms into its hadronic components ($\rho, \omega, \phi, J/\psi, \Upsilon$). Thus, a likely signal of the QED mechanism would be a vector meson going in one direction and a hadronic system going in the opposite direction, with a large rapidity gap in between. Events containing a narrow resonance such as the J/ψ recoiling against a dijet system could be particularly interesting since the direction and polarization of the vector meson is revealed through its decay into a lepton pair. Combining with beam polarization, the detailed study of these events can offer non-trivial tests of Standard

Model features. Monte Carlo study of the hadronization stage [3] would allow us to distinguish the gap events produced through the described mechanisms from the random fluctuation of hadron fragments. Finally, let us point out that at future linear colliders (energies above the Z mass) the QED-induced rapidity gap events can also come from configurations corresponding to the "radiative tail" of the Z. That is, a low mass photon emitted in the initial state takes away the right amount of energy to "restore" the virtual Z into resonance, and two color singlet jet-systems are generated separately as the decay products of the virtual photon and the resonant Z.

ACKNOWLEDGEMENTS

We thank James D. Bjorken for helpful discussions.

REFERENCES

[1] J. D. Bjorken, S. J. Brodsky and H. J. Lu, Phys. Lett. **B286**, 153 (1992).

[2] J. Randa, Phys. Rev. **D21**, 1795 (1980).

[3] Monte Carlo simulations of QCD rapidity gap events and their backgrounds at the SLC are now underway. (Phil Burrows, private communication.)

[4] Yu.L. Dokshitzer, V.A. Khoze and S.I.Troyan, in Proc. Sixth Intern. Conf. on Physics in Collision (1986), ed. M. Derrick (World Scientific, Singapore, 1987) p. 417. Yu.L. Dokshitzer, V.A. Khoze and T. Sjöstrand, Phys. Lett. **B274**, 116 (1992).

[5] J. D. Bjorken, Phys. Rev. **D47**, 101 (1992), Int. J. Mod. Phys. **A7**, 4189 (1992).

[6] H. Chehime, M.B. Gay Ducati, A. Duff, F. Halzen, A.A. Natale, T. Stelzer and D. Zeppenfeld, Phys. Lett. **B286**, 397 (1992). R.S. Fletcher and T. Stelzer, BA–92–43 (1992). V. Del Duca and W.-K. Tang, SLAC–PUB–6095 (1993). H. Chehime and D. Zeppenfeld, MAD–PH–725 (1992), MAD–PH–748 (1993). E. Gotsman, E.M. Levin and U. Maor, TAUP–2030–93 (1993). E. Levin, FERMILAB–PUB–93–012–T (1993).

[7] V. N. Baier, V. S. Fadin, V. A. Khoze and E.A. Kuraev, Phys. Rept. **78**, 294 (1981). R. N. Cahn, Phys. Rev. **D36**, 2666 (1987). J. P. Alexander, G. Bonvicini, P. S. Drell and R. Frey, Phys. Rev. **D37**, 56 (1988).